J. Fluid Mech. (1997), *vol.* 343, *pp.* 111–130. Printed in the United Kingdom

Direct numerical simulations of passive scalars with $Pr > 1$ advected by turbulent flow

By DAREK BOGUCKI[1], J. ANDRZEJ DOMARADZKI[1] AND P. K. YEUNG[2]

[1]Department of Aerospace Engineering, University of Southern California, Los Angeles, CA 90089-1191, USA

[2]School of Aerospace Engineering, Georgia Institute of Technology, Atlanta, GA 30332-0150, USA

(Received 24 January 1996 and in revised form 10 February 1997)

Direct numerical simulations of passive scalars, with Prandtl numbers $Pr = 3, 5$, and 7, advected by turbulence at three low Reynolds numbers were performed. The energy spectra are self-similar under the Kolmogorov scaling and exhibit behaviour consistent with many other investigations: a short inertial range for the highest Reynolds number and the universal exponential form of the spectrum for all Reynolds numbers in the dissipation range. In all cases the passive scalar spectra collapse to a single self-similar curve under the Batchelor scaling and exhibit the k^{-1} range followed by an exponential fall-off. We attribute the applicability of the Batchelor scaling to our low-Reynolds-number flows to the universality of the energy dissipation spectra. The Batchelor range is observed for wavenumbers in general agreement with experimental observations but smaller than predicted by the classical estimates. The discrepancy is caused by the fact that the velocity scales responsible for the generation of the Batchelor range are in the vicinity of the wavenumber of the maximum energy dissipation, which is one order of magnitude less than the Kolmogorov wavenumber used in the classical theory. Two different functional forms of passive scalar spectra proposed by Batchelor and Kraichnan were fitted to the simulation results and it was found that the Kraichnan model agrees very well with the data while the Batchelor formula displays systematic deviations from the data. Implications of these differences for the experimental procedures to measure the energy and passive scalar dissipation rates in oceanographic flows are discussed.

1. Introduction

The spectral behaviour of kinetic energy spectra in homogeneous isotropic turbulence is fairly well established through results from experiments, theoretical studies, and numerical simulations. These studies have been reviewed in several monographs (Monin & Yaglom 1971; Lesieur 1990). For flows at high Reynolds numbers the most important part of the spectrum is the $k^{-5/3}$ inertial subrange, which according to the Kolmogorov (1941) theory terminates below the Kolmogorov or dissipation wavenumber

$$k_K = (\epsilon/\nu^3)^{1/4} = 1/\eta_K, \tag{1}$$

where ϵ is the kinetic energy dissipation rate, ν is the kinematic viscosity, and η_K is the Kolmogorov length scale. Experimental results indicate that the inertial range ends at

wavenumbers lower than or around $k \approx (0.1-0.2)k_K$. Many theoretical and numerical results (Kraichnan 1959; Kerr 1990; Domaradzki 1992; Chen *et al.* 1993; Martinez *et al.* 1996) support the following form for the dissipation range for wavenumbers $k > 0.2k_K$:

$$E(k) \sim (k/k_K)^{\alpha} \exp(-ak/k_K). \tag{2}$$

The exponential is well established and has been confirmed by the experiments of Sreenivasan (1985) but the algebraic prefactor is uncertain though several investigations suggest $\alpha \approx -2$ in the range $0.2 < k/k_K < 4$. While the inertial subrange exists only for sufficiently high-Reynolds-number turbulence, generally inaccessible to numerical simulations, the dissipation-range form (2) appears to be universally valid for all Reynolds numbers and can be easily simulated numerically. The universality in particular implies that those features of turbulence that are determined by scales from the vicinity of k_K can be investigated through direct numerical simulations (DNS) irrespective of Reynolds number. This observation is used later in our work.

In many physical situations one encounters passive scalars advected by turbulent velocity fields like temperature and pollutants in air and water. Following Kolmogorov's local isotropy hypothesis Obukhov (1949) and Corrsin (1951) predicted that scalar variance spectra at high Reynolds numbers will also have a $k^{-5/3}$ inertial subrange. The behaviour of the variance spectra for wavenumbers beyond the Corrsin–Obukhov range depends on the Prandtl (or Schmidt) number $Pr = \nu/\kappa$, where κ is the scalar diffusivity. For $Pr < 1$ Batchelor, Howells & Townsend (1959) predict the following form for the spectrum of the variance of a scalar advected by the velocity scales from the inertial subrange:

$$E_\theta(k) \sim \chi \kappa^{-3} \epsilon^{2/3} k^{-17/3}, \tag{3}$$

where χ is the scalar variance dissipation rate; the formula is valid for wavenumbers k greater than the Obukhov–Corrsin wavenumber

$$k_{OC} = (\epsilon/\kappa^3)^{1/4} = Pr^{3/4} k_K. \tag{4}$$

Following Batchelor *et al.*'s (1959) assumptions Chasnov, Canuto & Rogallo (1988) performed numerical simulations of a passive scalar advected by a frozen velocity field with the inertial-range spectrum as well as by a velocity field obtained in large-eddy simulations. In both cases the spectral form (3) was observed.

In oceanographic applications temperature and salinity are important scalars, and both have $Pr > 1$. The case of $Pr \gg 1$ was investigated theoretically by Batchelor (1959) who derived the following form of the scalar spectrum in the viscous–convective range:

$$E_\theta(k) = -(\chi/\gamma) k^{-1} \exp(\kappa k^2/\gamma), \tag{5}$$

where γ is the average value of the least principal rate of strain (a negative quantity) acting on scales $k > k_K$. The derivation is based on a physical picture of the scalar field at scales $k \gg k_K$ being deformed by an essentially uniform gradient of the velocity at much larger scales $k \approx k_K$. For k less than the Batchelor wavenumber

$$k_B = (\epsilon/\nu\kappa^2)^{1/4} = Pr^{1/2} k_K = 1/\eta_B, \tag{6}$$

the exponential factor in (5) is approximately equal to unity and the algebraic prefactor k^{-1} dominates such that the so-called Batchelor spectrum becomes

$$E_\theta(k) = -(\chi/\gamma) k^{-1}. \tag{7}$$

The final form of the Batchelor spectrum is determined by specifying the strain rate

γ. For flows at high Reynolds numbers it is assumed that a good estimate is given by the rate of strain of Kolmogorov eddies

$$\gamma = -(1/q)(\epsilon/\nu)^{1/2}, \tag{8}$$

where q is a universal constant. Using available experimental data Batchelor (1959) estimated $q \approx 2$. Gibson (1968*b*) provides a range of values $\sqrt{3} < q < 2\sqrt{3}$ deduced from the incompressibility and kinematics of fluid elements. Oceanic measurements provided values of $q = 3.9 \pm 1.5$ (Grant *et al.* 1968) and $q = 3.7 \pm 1.5$ (Oakey 1982).

Each of the previous spectral predictions for scalar spectra results from a separate set of physical assumptions, making the predictions independent of each other. Gibson (1968*a*, *b*) proposed a unified theory of passive scalars advected by turbulence valid for all values of the Prandtl number. The theory is based on the physical mechanism of generation of maxima and minima of the scalar concentration by the local rates of strain. This mechanism is distinctly different from the mechanism invoked by Batchelor for $Pr \gg 1$. While for $Pr > 1$ Gibson's prediction for the spectra of the scalar is the same as Batchelor's prediction (5), for $Pr \ll 1$ Gibson's theory implies the intermediate k^{-3} range for $k_{OC} < k < k_B$ before the $k^{-17/3}$ range develops for $k > k_B$. The evidence in support of Gibson's theory is discussed by Clay (1973), and Kerr (1990). In the context of our work Gibson's analysis has two appealing features. First, it suggests that the Batchelor k^{-1} range may appear even if the Prandtl number is not much greater than unity (i.e. the condition $Pr > 1$ replaces Batchelor's $Pr \gg 1$). Second, it implies a universal scaling independent of the Prandtl number for scalar spectra in the scalar dissipation range. This so-called Batchelor scaling is obtained by normalizing wavenumbers by the Batchelor length scale η_B and spectra by $\chi(\nu/\epsilon)^{1/2}\eta_B$. Under this scaling expression (5) is given by a self-similar form

$$\frac{E_\theta(k\eta_B)}{\chi(\nu/\epsilon)^{1/2}\eta_B} = q(k\eta_B)^{-1}\exp(-q(k\eta_B)^2). \tag{9}$$

Kraichnan (1968) considered the effects of fluctuations of the rates of strain in space and time in Batchelor's analysis and showed that while k^{-1} behaviour survives, the Gaussian factor in (5) is not universal and is replaced by a simple exponential. He also obtained the same result using Lagrangian-history-direct-interaction (LDHI) closure theory. Kraichnan's equation for a scalar spectrum was solved in a closed form by Mjølsness (1975) giving the following result:

$$E_\theta(k) = 5(\chi/\Lambda)k^{-1}(1+\xi)\exp(-\xi), \tag{10}$$

where $\xi = (30\kappa/\Lambda)^{1/2}k$, and the constant Λ can be in principle calculated from the theory. By comparing functional expressions (10) and (7) in the limit $k \to 0$ we get $\Lambda = (5/q)(\epsilon/\nu)^{1/2}$. Using the Batchelor scaling formula (10) becomes

$$\frac{E_\theta(k\eta_B)}{\chi(\nu/\epsilon)^{1/2}\eta_B} = q(k\eta_B)^{-1}(1+(6q)^{1/2}k\eta_B)\exp(-(6q)^{1/2}k\eta_B). \tag{11}$$

Similar expressions, containing the k^{-1} range and the exponential form, are also predicted by other analytical theories of turbulence (Newman & Herring 1979; Herring & Kerr 1982; Qian 1995). The analytical theories also make predictions about the universal constant q in (11). Kraichnan (1968) estimates $q < 0.9$ using LHDIA, Newman & Herring (1979) give $q = 1.68$ using the test field model and Qian (1995) gives $q = 2\sqrt{5}$. Only the last value is consistent with the experimental evidence.

In summary the classical picture of the scalar spectrum in high-Reynolds-number flow and $Pr \gg 1$ as uniformly presented in turbulence literature (Tennekes & Lumley 1972; Monin & Yaglom 1971; Lesieur 1990) is the inertial $k^{-5/3}$ behaviour for $k \ll k_K$, the Batchelor k^{-1} behaviour for $k_K < k < k_B$, and exponential decay for $k > k_B$.

Despite the wealth of theoretical results in favour of this picture the experimental evidence is ambiguous, ranging from supporting to rejecting in part or entirely the spectral forms, in particular the k^{-1} Batchelor range, arrived at by theoretical considerations. Gibson & Schwarz (1963) observed the Batchelor spectrum for temperature and salinity in laboratory measurements in water and the approximate k^{-1} behaviour for the temperature spectrum is also suggested by oceanographic field measurements of Grant *et al.* (1968), Clay (1973), and Oakey (1982). However, later measurements of Gargett (1985) contradicted the universality of the Batchelor spectrum and cast doubt on earlier experimental results. The oceanographic implications of this discrepancy are summarized in the review of Gregg (1987). More recently Miller & Dimotakis (1995) reported results of laboratory measurements of scalar spectra for high Schmidt number ($\simeq 1.9 \times 10^3$) in a turbulent jet which do not show any evidence of the k^{-1} spectral behaviour. Note that according to the Batchelor theory the large value of Schmidt number ($\gg 1$) in this experiment should allow for an easy detection of the k^{-1} range. Earlier Dimotakis & Miller (1991) showed that in the limit of infinite Schmidt numbers the scalar variance must remain bounded while it is well known that it diverges if the k^{-1} spectrum is assumed. The k^{-1} range is also absent in the high-Schmidt-number two-dimensional mixing experiments of Williams, Marteau & Gollub (1997). Thus some of the above results contradict the classical picture of high-Prandtl-number mixing but no single, satisfactory explanation of the observed departures from the k^{-1} behaviour is currently available. Several explanations have been proposed. Batchelor (1959) recognized the scalar variance divergence for high Schmidt numbers and suggested that the k^{-1} range may not be observed if there is not a sufficient flux of the scalar variance from the large scales to the small scales. Gibson (1991) attributes the departures from the Batchelor predictions in experiments to turbulence intermittency and fossilization. Williams *et al.* (1997) observe that the passive scalar may be trapped inside long-lived coherent vortices in two-dimensional turbulence resulting in dynamics inconsistent with the original assumptions of Batchelor.

In addition, when the Batchelor range is in fact observed the quality of the experimental data often does not allow a clear distinction between the spectral forms (11) and (9) in the far dissipation range. Consequently experimental results usually are interpreted assuming the earlier derived Batchelor spectrum (9) and no comparison studies with the Kraichnan spectrum are available. The practical importance of these spectral expressions lies in the fact that all scalar fluctuations and scalar dissipation are effectively determined by scales from the k^{-1} Batchelor range. The dissipation rates in turn determine the mixing coefficients for scalars (Dillon & Caldwell 1980) which are critical to understand the small-scale physics of the oceans as well as the large-scale circulation and global climate. Knowledge of spatial power spectra of temperature fluctuations at small scales is also needed to address problems of sound and light propagation in water (Tatarski 1961). Several scalar models have been examined for those problems (Hill 1978) but again lack of experimental data at the largest wavenumbers introduces uncertainties in the analyses. In view of the practical importance of the Batchelor spectrum and the scatter in the predicted values of the universal constant q as well as experimental controversies concerning the existence

of the k^{-1} range itself, further work in this area is clearly needed. Carefully designed numerical simulations may complement experiments and theory in contributing to the resolution of these controversies.

While numerical simulations have been used extensively to investigate scalar spectra for $Pr \leqslant 1$ (Kerr 1990; Ruetsch & Maxey 1991; Pumir 1994) no similar numerical effort has been devoted to the case of $Pr > 1$. The numerically discouraging aspect of this case is that substantially higher resolution is needed to simulate the scalar field than the velocity field. Indeed, the theoretically suggested location of the Batchelor spectrum, $k > k_K$, implies that the simulations should extend far into the dissipation range to values of $k \gg k_K$. This effectively limits the turbulence simulations on current supercomputers to very low values of the Reynolds number. However, two observations suggest that it may be possible to obtain the Batchelor spectrum in a properly designed numerical experiment despite the inability of DNS to simulate high-Reynolds-number flows. First, as already argued by Batchelor (1959) the form of the relation (5) should also hold for low-Reynolds-number flows, as long as $Pr \gg 1$ and there exist large velocity scales providing uniform rates of strain. More generally, the existence of the Batchelor range for scalars with $Pr \gg 1$ can be viewed as a consequence of the scalar diffusion in a strain field that is spatially fairly uniform and random. This is persuasively demonstrated by the simple physical model of Antonsen, Fan & Ott (1995) where the extensive k^{-1} range was obtained by numerically solving the passive scalar equation with the velocity field prescribed as a long monochromatic wave with a random phase. A similar approach has been employed by Holzer & Siggia (1994) for two-dimensional flows and by Pumir (1994) for three-dimensional flows. In both cases only a few low-wavenumber velocity modes, i.e. large scales, actively advect the passive scalar which is allowed to develop scales much smaller than the forcing velocity field. Holzer & Siggia (1994) observed the k^{-1} range for simulations performed with 512^2 modes and hyperdiffusion while Pumir (1994) estimates that in three dimensions the resolution of 1000^3 modes would be needed to observe the k^{-1} range. Also Metais & Lesieur (1992) attribute an 'anomalous' k^{-1} passive scalar range in their large-eddy simulations to stirring of temperature by the large energy-containing eddies. While in many of these cases the k^{-1} range is observed, the prevailing rate of strain γ in (7) is generally different from the estimate (8), expected to hold only for high-Reynolds-number turbulence. Second, as noted above, there is evidence that the energy dissipation range (2) is independent of (or only weakly dependent on) the Reynolds number. Therefore, the spectral dynamics of scales from the vicinity of the Kolmogorov wavenumber k_K, where the dissipation range is located, should be the same for large- and small-Reynolds-number flows. When Kolmogorov scaling is used the increase in the Reynolds number only extends the energy spectrum to smaller wavenumbers without affecting scales from the vicinity of the Kolmogorov scale. Since Batchelor theory assumes that the scalar variance dynamics is driven by the Kolmogorov velocity scales, the universality of the energy dissipation spectra implies that the velocity field for a low-Reynolds-number turbulent flow should have the same effect on the scalar in the Batchelor range as a high-Reynolds-number flow. This observation suggests that it is plausible to expect not only the same k^{-1} spectral behaviour, but also the same scaling, in particular for γ, to hold for all Reynolds numbers. Note, however, that previous numerical simulations performed for this problem (Holzer & Siggia 1994; Pumir 1994; Antonsen *et al.* 1995) deliberately did not attempt to simulate the dissipation range of the velocity field and thus were unable to address this issue.

In view of these arguments we believe that it is worthwhile to explore the dynamics

of passive scalars for $Pr > 1$ in low-Reynolds-number turbulent flows by numerically solving the full Navier–Stokes equation for velocity and a passive scalar.

2. Basic equations and numerical methods

The flow dynamics are described by the incompressible Navier–Stokes equations for velocity $\boldsymbol{u}(\boldsymbol{x}, t)$ and the transport equation for the passive scalar $\theta(\boldsymbol{x}, t)$

$$\frac{\partial \boldsymbol{u}}{\partial t} + (\boldsymbol{u} \cdot \nabla)\boldsymbol{u} = -\frac{1}{\rho}\nabla p + \nu \nabla^2 \boldsymbol{u} + \boldsymbol{F}_u, \tag{12}$$

$$\nabla \cdot \boldsymbol{u} = 0, \tag{13}$$

$$\frac{\partial \theta}{\partial t} + (\boldsymbol{u} \cdot \nabla)\theta = \kappa \nabla^2 \theta + F_\theta. \tag{14}$$

In the equations ρ is a constant density, p is the pressure, and ν and κ are the kinematic viscosity and the molecular diffusivity, respectively. The terms $\boldsymbol{F}_u$ and F_θ signify forcing added to the equations in order to obtain statistically stationary turbulence.

The flow is assumed to be contained in a cube of side $L = 2\pi$ and periodic boundary conditions in all three spatial directions are imposed on the independent variables. The domain is discretized in physical space using N uniformly spaced grid points in each direction resulting in a mesh size $\Delta x = L/N$ and a total of N^3 grid points. The equations of motion are transformed to spectral space using the discrete Fourier transform

$$\boldsymbol{u}(\boldsymbol{k}) = \frac{1}{N^3} \sum_{\boldsymbol{x}} u(\boldsymbol{x}) \exp(-\mathrm{i}\boldsymbol{k} \cdot \boldsymbol{x}), \tag{15}$$

and the inverse transform is

$$\boldsymbol{u}(\boldsymbol{x}) = \sum_{\boldsymbol{k}} u(\boldsymbol{k}) \exp(\mathrm{i}\boldsymbol{k} \cdot \boldsymbol{x}), \tag{16}$$

where $\boldsymbol{x}$ are the mesh points in physical space and $\boldsymbol{k}$ are the discrete wavenumbers with components $k_i = \pm n_i \Delta k$, $n_i = 0, 1, 2, ...N/2$, $i = 1, 2, 3$, and $\Delta k = 2\pi/L = 1$. The distinction between physical and spectral representation for a given quantity is made through its argument $\boldsymbol{x}$ or $\boldsymbol{k}$, respectively.

The equations are solved using a pseudo-spectral numerical method of Rogallo (1981) in the implementation of Yeung & Pope (1988). We have employed the forcing scheme of Sullivan, Mahalingam & Kerr (1994) in which the total energy of several low-wavenumber modes is kept constant while evolution of individual modes through nonlinear interactions, subject to the global constraint, is allowed. Specifically, the sum of squared amplitudes of modes in a sphere of radius $K_f = 2.5\Delta k$ is kept constant for both the velocity and the passive scalar. This is accomplished by multiplying all modes in the forced sphere by the same constant factor, usually not larger than 1.02, at the end of each time step. This restores the energy (or the scalar variance) in the sphere to the value at the beginning of the time step.

Physical quantities of interest for isotropic turbulence are described in terms of the scalar wavenumber $k = |\boldsymbol{k}|$ by averaging over thin spherical shells defined for an arbitrary quantity $f(\boldsymbol{k})$ as

$$\langle f(\boldsymbol{k}) \rangle = \frac{1}{N_{\boldsymbol{k}}} \sum_{\boldsymbol{k}} f(\boldsymbol{k}), \tag{17}$$

where $\langle ... \rangle$ denotes the shell average and the summation extends over all $N_{\boldsymbol{k}}$ modes in the shell of thickness Δk centred at $k = |\boldsymbol{k}|$. The energy and the passive scalar spectra are defined as follows

$$E(k) = 4\pi k^2 \langle \tfrac{1}{2} u_n(\boldsymbol{k}) u_n^*(\boldsymbol{k}) \rangle, \tag{18}$$

$$E_\theta(k) = 4\pi k^2 \langle \theta(\boldsymbol{k}) \theta^*(\boldsymbol{k}) \rangle, \tag{19}$$

and the corresponding dissipation spectra are

$$D(k) = 2\nu k^2 E(k), \tag{20}$$

$$D_\theta(k) = 2\kappa k^2 E_\theta(k). \tag{21}$$

The integral of $E(k)$ over k gives turbulent kinetic energy per unit mass $3/2\overline{u^2} = 3/2u'^2$, where the overbar denotes averaging in physical space and u' is the r.m.s. turbulent velocity, and the integral of $E_\theta(k)$ gives the scalar variance $\overline{\theta^2}$. The integrated dissipation spectra give the dissipation rates of the kinetic energy, ϵ, and of the scalar, χ. The Taylor microscale is computed as $\lambda = (15u'^2\nu/\epsilon)^{1/2}$ and the microscale Reynolds number is $R_\lambda = u'\lambda/\nu$. An important time scale for the evolution of turbulence is the large-eddy turnover time $T_e = L_p/u'$, where L_p is the integral length scale

$$L_p = \frac{\pi}{2u'^2} \int_0^\infty k^{-1} E(k) \mathrm{d}k. \tag{22}$$

L_p is used to define the macroscale Reynolds number $Re = u'L_p/\nu$ and the Péclet number $Pe = u'L_p/\kappa = Pr\,Re$.

Values of the velocity-derivative skewness S_u and the mixed-derivative skewness $S_{u\theta}$ are often used in direct numerical simulations to assess how well turbulence is developed. The velocity derivative skewness S_u is given by the formula

$$S_u = \frac{\langle \left(\partial u_1/\partial x_1\right)^3 \rangle}{\langle \left(\partial u_1/\partial x_1\right)^2 \rangle^{3/2}}. \tag{23}$$

For isotropic turbulence the vorticity production rate is proportional to the velocity-derivative skewness S_u. The mixed-derivative skewness $S_{u\theta}$

$$S_{u\theta} = \frac{\langle \left(\partial u_1/\partial x_1\right) \left(\partial \theta/\partial x_1\right)^2 \rangle}{\langle \left(\partial u_1/\partial x_1\right)^2 \rangle^{1/2} \langle \left(\partial \theta/\partial x_1\right)^2 \rangle}, \tag{24}$$

is related to the nonlinear transfer of scalar variance to small scales and takes a value zero when there is no net cascade to higher wavenumbers. For statistically steady isotropic turbulence S_u and $S_{u\theta}$ may be expressed entirely in terms of energy and passive scalar spectra (Kerr 1985)

$$S_u = 2.35\nu \frac{\int k^4 E(k) \mathrm{d}k}{(\epsilon/15\nu)^{3/2}}, \tag{25}$$

$$S_{u\theta} = \frac{2}{15}\kappa \frac{\int k^4 E_\theta(k) \mathrm{d}k}{(\epsilon/15\nu)^{1/2}\,(\chi/6\kappa)}. \tag{26}$$

Run	Resolution	ν	k_{max}	L_p	λ	η_K	u'	ϵ	R_λ	Re	$-S_u$
x162	162^3	0.02	76	1.55	$\simeq 1.1$	0.111	0.44	0.052	$\simeq 25$	34	0.60
aa162	162^3	0.01	76	1.34	$\simeq 0.8$	0.0680	0.47	0.047	$\simeq 36$	62	0.46
a240	240^3	0.0033	113	1.09	$\simeq 0.4$	0.0259	0.56	0.080	$\simeq 77$	185	0.51

TABLE 1. Parameters of the simulations for the velocity field.

3. Results

Calculations were carried out on the Cray C90 with resolution of up to 240^3 modes. In addition to the turbulent velocity field in each run we carried three passive scalars with values of the Prandtl number of 3, 5, and 7. The low-wavenumber modes for both velocity and scalars were forced as described earlier. As an initial condition we used the prescribed energy spectrum proportional to the exponential $E(k,0) = C\exp(-ck)$, where constants C and c were chosen for a given resolution to provide a prescribed value of the microscale Reynolds number. This form of the initial conditions is consistent with the experimental fall-off of the dissipation spectra at larger wavenumbers (2). Since low-wavenumber modes $0 < k \leqslant K_f = 2.5\Delta k$ are forced and excluded from the analysis, we did not attempt to match in the initial conditions the algebraic prefactor in (2). Equivalently, we could have initialized simulations with a constant energy spectrum for the forced modes $k \leqslant K_f$ and vanishing spectrum for $k > K_f$, but such simulations would require longer time to reach a statistically stationary state. The initial scalar spectra were proportional to the energy spectrum. The simulations were started with the resolution of 128^3 modes and run for about one large-eddy turnover time. Subsequently, the generated dataset was used as a restart for a run at higher resolution 162^3 which was allowed to evolve until a steady state for the scalar field was achieved (it takes longer for the scalar spectra to achieve equilibrium than for the energy spectra (Pumir 1994)). In this procedure at the restart time the high-wavenumber modes, outside the initial (smaller) spectral domain, are all zero. After the restart these modes evolve rapidly as they gain energy from the modes in the original smaller spectral domain by the nonlinear interactions. The change in the Reynolds number was accomplished by changing the viscosity. We found that this approach in increasing resolution minimizes the CPU time needed to generate a fully developed, statistically steady spectrum at the target resolution while still generating proper results. Turbulence parameters in all runs were chosen such that all energy and scalar spectra are well resolved in the final state. Owing to computer time constraints the highest resolution case was run for about one large-eddy turnover time after restarting from one of the 162^3 runs. Towards the end of this run the high-wavenumber modes, initially zero at the restart time, still experience slight energy increase indicating imbalance between the nonlinear transfer and the dissipation in this part of the spectrum. However, the remaining parts of the spectrum are found in statistical equilibrium, and the velocity-derivative skewness and the mixed-derivative skewness for this run attain generally accepted equilibrium values. These observations imply that simulated turbulence is sufficiently well developed for the purpose of our analysis which focuses on the k^{-1} behaviour at low wavenumbers. Only results from the simulations performed with the higher resolutions of 162^3 and 240^3 modes are reported here. Parameters for these runs are collected in tables 1 and 2.

Results for the spectra presented below are calculated using shell averages (17) with the first two forced shells removed and are suitably non-dimensionalized, bringing

Run	Pr	η_B	χ	Pe	$-S_{u\theta}$
	3	0.064	0.17	102	0.45
x162	5	0.050	0.16	170	0.42
	7	0.042	0.16	238	0.45
	3	0.040	0.16	186	0.38
aa162	5	0.030	0.19	310	0.40
	7	0.026	0.16	434	0.38
	3	0.015	0.26	555	0.41
a240	5	0.012	0.26	925	0.39
	7	0.0098	0.27	1295	0.36

TABLE 2. Parameters of the simulations for the scalar field.

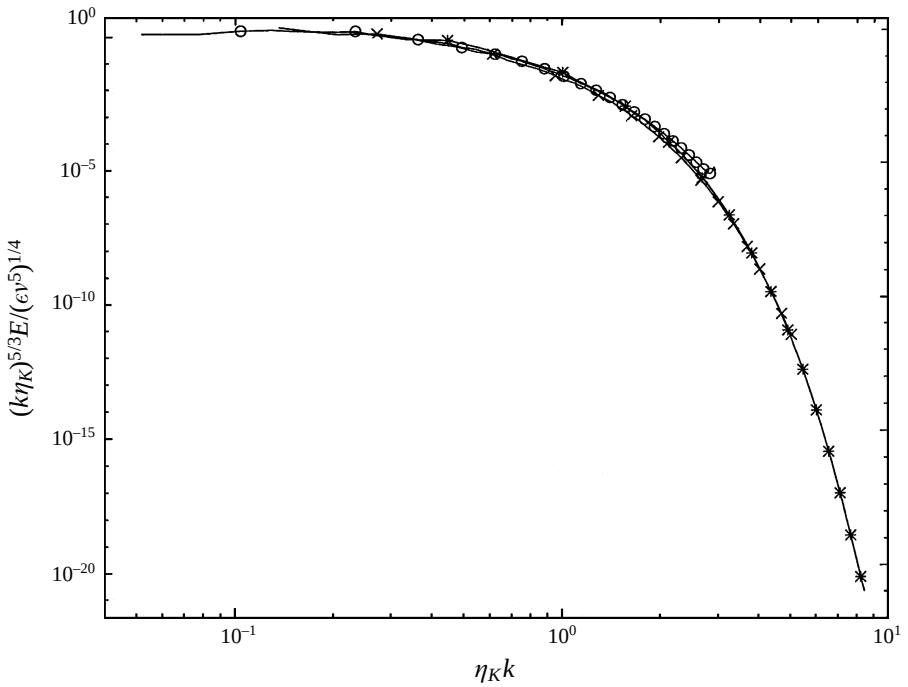

FIGURE 1. Normalized energy spectra $E(k\eta_K)(k\eta_K)^{5/3}/(\epsilon\nu^5)^{1/4}$ for all runs (×, run aa162; ○, run a240; ∗, run x162).

data from all runs to a self-similar form. The classical Kolmogorov scaling procedure for the energy spectra (Kerr 1990) uses η_K and $(\epsilon\nu^5)^{1/4}$ for non-dimensionalization of wavenumbers and spectra, respectively. For scalar spectra the Batchelor (1959) scaling is usually employed where η_B and $\chi(\nu/\epsilon)^{1/2}\eta_B$ are used to non-dimensionalize wavenumber k and the spectra, respectively.

3.1. *The velocity spectra*

Figure 1 presents a log-log plot of three-dimensional energy spectra using the Kolmogorov scaling and multiplied by $(k\eta_K)^{5/3}$. For wavenumbers $k\eta_K < 0.2$ the plotted functions appear flat which suggests a 5/3 slope for the energy spectra characteristic

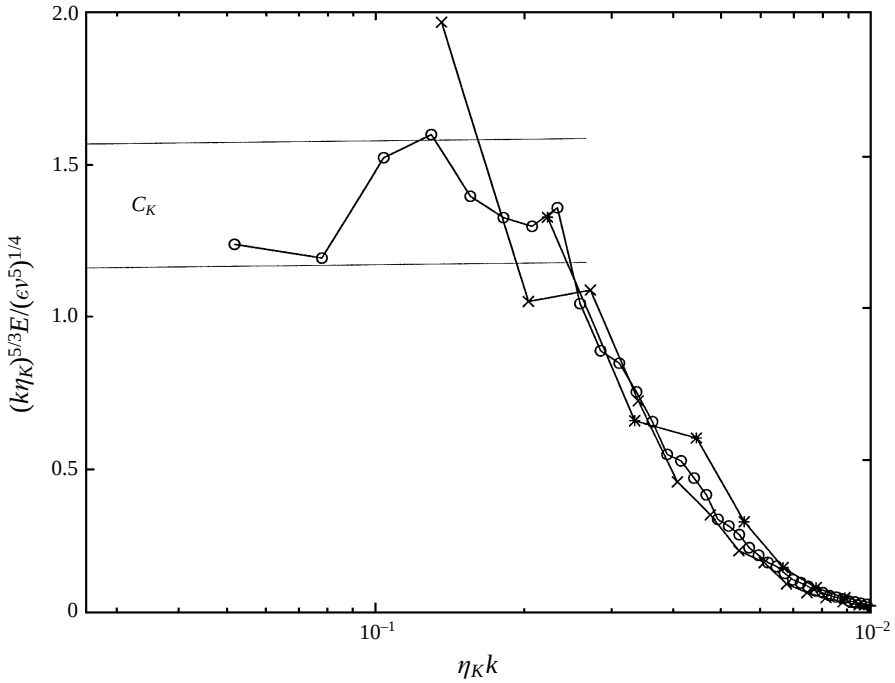

FIGURE 2. Normalized energy spectra $E(k\eta_K)(k\eta_K)^{5/3}/(\epsilon\nu^5)^{1/4}$ in the range of low wavenumbers. The horizontal lines in the plot mark the range of values of the Kolmogorov constant (symbols as figure 1).

of the inertial range. This range of small wavenumbers is enlarged in figure 2 where the vertical axis is plotted using a linear scale. The approximate inertial range is clearly present in run a240 where the Kolmogorov constant C_K is between 1.2 and 1.6 for $k\eta_K < 0.2$. This value is consistent with the values observed experimentally but smaller than reported in numerical simulations where values around 2.0 are frequently found. No inertial-range behaviour is found for runs at lower Reynolds numbers. It is also clear that the Kolmogorov scaling succeeds in bringing spectra at different Reynolds numbers into a self-similar form. The values of the velocity-derivative skewness S_u for all runs are given in table 1 and are consistent with the generally accepted value of -0.5 (Kerr 1985) for well-developed turbulence. Figure 3 presents the same quantity as in the previous figures but plotted on the log-linear scale which emphasizes the far dissipation range. In the far dissipation range the energy spectrum is believed to be a simple exponential, i.e $E(k) \sim B\exp(-a\eta_K k)$. Our data give value of $B = 8.5$ and $a = 5.4$ consistent with values of $B = 8.4 \pm 0.6$ and $a = 5.1 \pm 0.1$ of Kida & Murakami (1987). This fit is particularly good for the coefficient B due to large resolution of our runs and relatively poorer for the slope a because of the early termination of the a240 run.

In figure 4 we plot the normalized kinetic energy dissipation spectra. In all cases the dissipation is concentrated at $k\eta_K$ around $(1\text{–}2)\times 10^{-1}$. For the highest resolution case we observe the well-defined dissipation peak but for the two cases at the lower resolution the maximum of the dissipation spectrum occurs at the smallest unforced wavenumbers. A complete overlap between the energy-containing and the dissipation ranges is consistent with the lack of the inertial subrange in the latter cases.

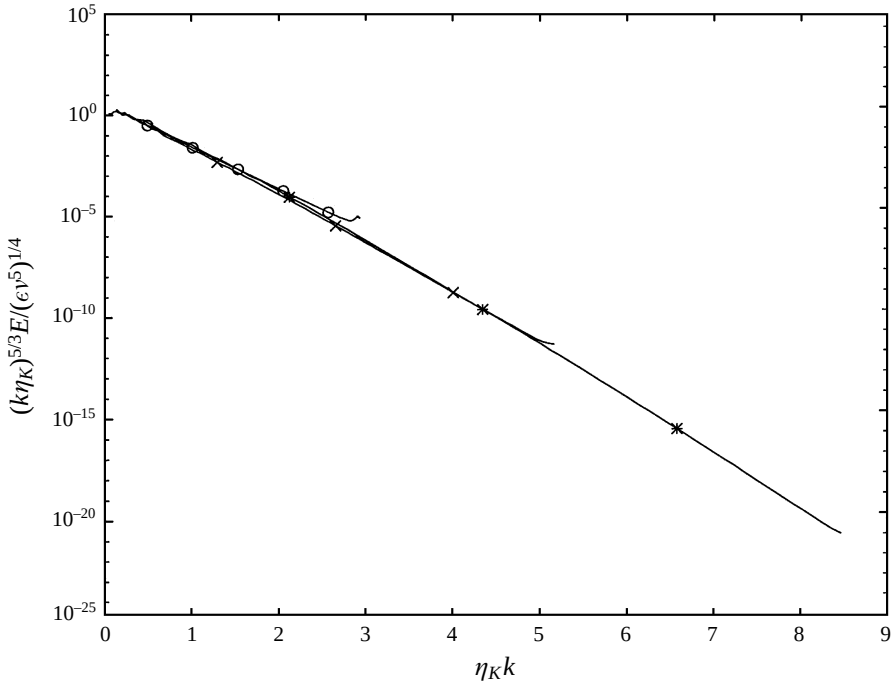

FIGURE 3. Normalized energy spectra $E(k\eta_K)(k\eta_K)^{5/3}/(\epsilon\nu^5)^{1/4}$ plotted using log-linear scale to emphasize the exponential form (symbols as figure 1).

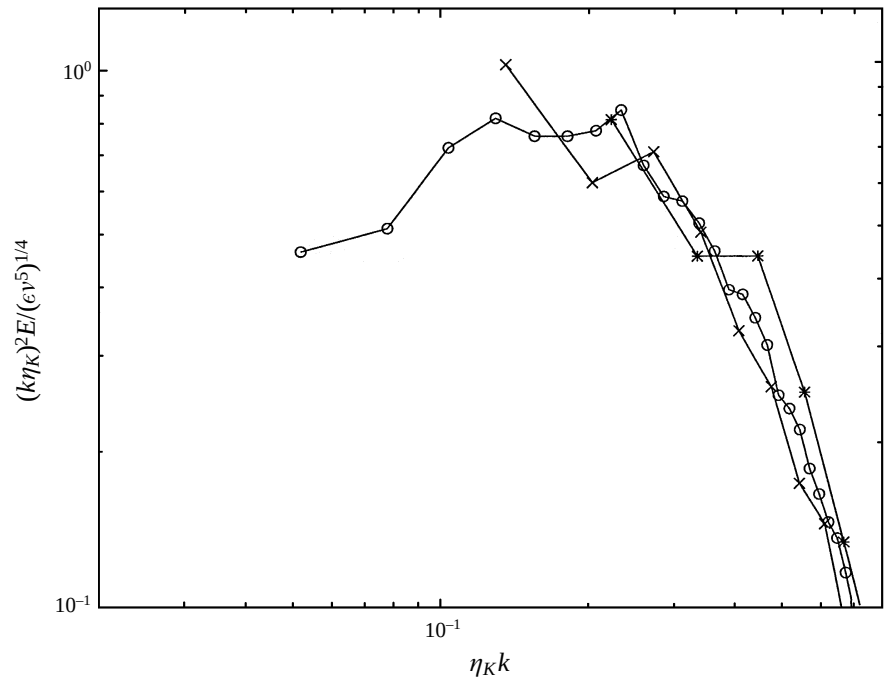

FIGURE 4. The normalized energy dissipation spectra $E(k\eta_K)(k\eta_K)^2/(\epsilon\nu^5)^{1/4}$ in the range of low wavenumbers (symbols as figure 1).

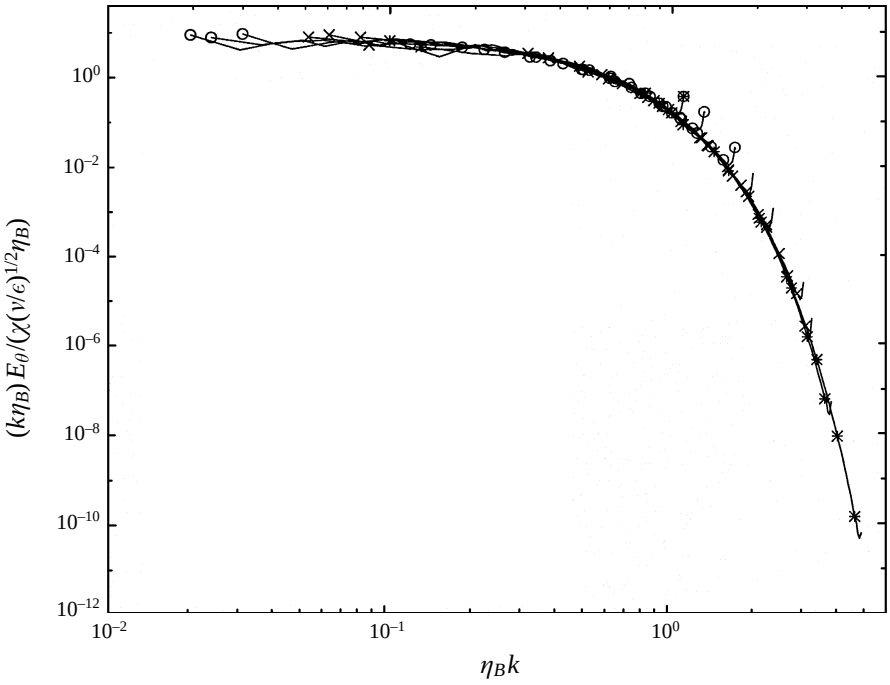

FIGURE 5. Normalized scalar spectra $E_\theta(k\eta_B)(k\eta_B)/(\chi(\nu/\epsilon)^{1/2}\eta_B)$ for all runs and all Prandtl numbers (symbols as figure 1).

3.2. *The scalar variance spectra*

In the previous subsection we showed that the energy spectra are self-similar and are consistent with other numerical and experimental results. This suggests that the numerically simulated velocity fields can be used to reliably advect passive scalars in order to study their dynamics. This suggestion is supported by the observed values of the mixed-derivative skewness $S_{u\theta}$ in the simulations. One of the secondary predictions of Gibson's (1968*b*) theory is that the mixed-derivative skewness is a constant independent of the Reynolds and Prandtl numbers. Numerical simulations of Kerr (1985, 1990) agree with this prediction giving $S_{u\theta} \simeq -0.5$. The mixed-derivative skewness is found to be around -0.4 in the experiments of Clay (1973). In our simulations $S_{u\theta}$ is close to -0.4 for all analysed runs (see table 2). This also implies that the interactions between the velocity and scalar are well developed in the final states analysed in this paper.

The controversial evidence for the existence of the Batchelor spectrum comes mostly from a few laboratory and oceanographic measurements and numerical solutions of simplified model problems (Caldwell *et al.* 1980; Oakey 1982; Gibson & Schwarz 1963; Holzer & Siggia 1994; Pumir 1994; Antonsen *et al.* 1995). To our knowledge there are no existing numerical simulations of full Navier–Stokes equations for passive scalar fields with $Pr > 1$ which exhibit the Batchelor-range behaviour.

In figure 5 we plot the scalar spectra multiplied by $k\eta_B$ using the Batchelor scaling for all three runs and all three Prandtl numbers $Pr = 3, 5, 7$. All curves collapse tightly to one universal form which shows that the Batchelor scaling is indeed universal for $Pr > 1$ in the dissipation and the far dissipation range.

Because of the multiplication by $k\eta_B$ the flat part of the curves in the range of small

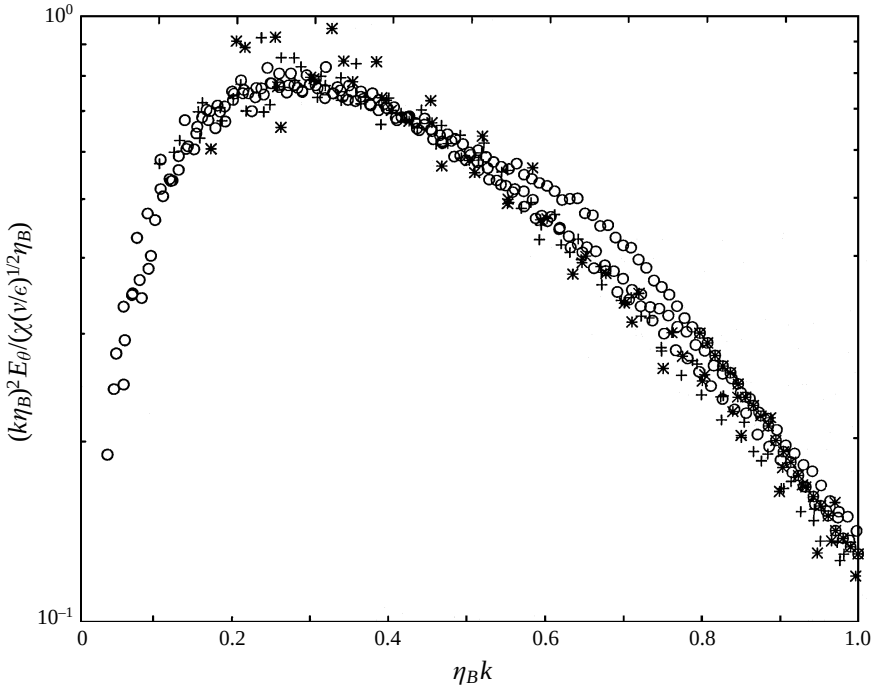

FIGURE 6. Normalized scalar dissipation spectra $E_\theta(k\eta_B)(k\eta_B)^2/(\chi(\nu/\epsilon)^{1/2}\eta_B)$ for all runs and all Prandtl numbers (symbols as figure 1).

wavenumbers $0.02 < k\eta_B < 0.2$ corresponds to the Batchelor-range k^{-1} behaviour which is observed in our simulations even for scalar with the Prandtl number as low as 3.

In figure 6 we plot the normalized dissipation spectra $E_\theta(k\eta_B)(k\eta_B)^2/(\chi(\nu/\epsilon)^{1/2}\eta_B)$ for all cases. The Batchelor scaling clearly collapses the dissipation spectra for all Reynolds numbers and Prandtl numbers and the location of the dissipation peak around $k\eta_B = 0.25$ is consistent with oceanic data of Oakey (1982).

3.3. *Parameters of the scalar spectra in the dissipation range*

In the spectral forms proposed by Batchelor (9) and by Kraichnan (11) the constant q is unknown while all other parameters are either prescribed (ν and κ) or can be computed from the data (ϵ and χ). Values of the universal constant q are obtained from the least-square fit of formulas (9) and (11) to the numerical data for run a240 giving $q_B = 3.9 \pm 0.25$ and $q_{Kr} = 5.26 \pm 0.25$, respectively. In figure 7 we present the results of the fit compared with the numerical data. Kraichnan's spectral form describes our data extremely well, with an exception in the exponential tail corresponding to the scalar with $Pr = 7$. This can be attributed to the previously discussed fact that in this case the scalar field still evolves in the range of the largest wavenumbers. In the case of the Batchelor form the best-fit curve (figure 7) shows large systematic deviation from our numerical data. The systematic deviations of the Batchelor prediction from experimental data measured *in situ* has long been noted in oceanographic literature. Oakey (1982) observed that in the k^{-1} portion of the spectrum the best fit to the Batchelor spectrum systematically under predicts the experimental data. We observe similar behaviour in our simulations (see figure 7),

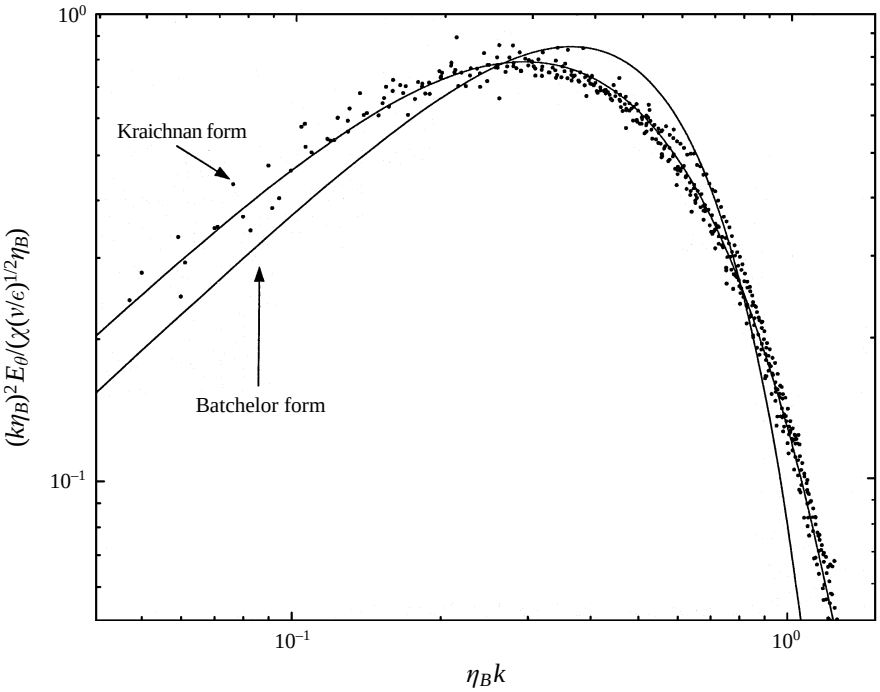

FIGURE 7. Normalized scalar dissipation spectra $E_\theta(k\eta_B)(k\eta_B)^2/(\chi(\nu/\epsilon)^{1/2}\eta_B)$ for run a240 and the best least-squares fit provided the Kraichnan and Batchelor spectral forms.

with the numerical data located above the Batchelor curve for wavenumbers before the dissipation peak. Our estimate of $q_B = 3.9$ is in good agreement with the value $q = 3.7 \pm 1.5$ obtained by Oakey (1982) from oceanic measurements.

Two different forms of passive scalar spectra (9) and (11) imply different error estimates for spectrally under-resolved experimental measurements of the scalar dissipation rate χ. The experimentally resolved wavenumbers usually do not extend beyond $k\eta_B \approx 1$. The scalar dissipation rate associated with wavenumbers greater than $k\eta_B \approx 1$ is 2% and 6% of the total dissipation rate for the Batchelor and Kraichnan forms, respectively. Thus the use of the Batchelor form would imply that error due to a limited extend of the spectra is on the order of only 2%. However, the much better fit of the Kraichnan form to the data implies that the wavenumbers in the range $k\eta_B > 1$ actually contribute about 6% to the total dissipation rate, and the measured χ should be corrected by this amount. Nevertheless, with the wavenumber resolution up to $k\eta_B \approx 1$ both spectral forms will result in values of χ within few percent of each other.

Sometimes in oceanographic experiments the kinetic energy dissipation rate ϵ is also determined indirectly from the measured temperature variance spectra. This is accomplished by assuming that the temperature spectra are properly described by the Batchelor formula (9) with the assumed value of the universal constant q. The temperature variance dissipation rate χ is computed directly from the measurements and ϵ is treated as a parameter whose value is specified by requiring the best least-squares fit of (9) to the measured data. We have attempted to estimate the sensitivity/error in such a procedure associated with using either the Batchelor or the Kraichnan model. Several subsets of our data set (run a240) were selected such that

the majority of the points belonged to either the pre-peak, peak or far dissipation range. In all sets the dissipation peak was resolved. Using earlier established optimum values of the constant q, q_{Kr}, and q_B, this procedure yielded the relative error in estimated values of η_B up to 6% when using the Batchelor form and an order of magnitude less in the Kraichnan form. Since $\epsilon \propto \eta_B^4$, fitting the Batchelor form to experimental data can account for at least 25% of the error in ϵ estimates. In the presence of systematic measurement noise the error is expected to be larger. Because of the much smaller error implied by the Kraichnan formula its use should be attempted in estimating the kinetic energy dissipation rates from the temperature variance measurements in oceanic environment.

Finally, in this context it may be noted that Gibson (1991) argues that the errors in estimating the dissipation rates from local measurements may be significantly larger if intermittence of turbulence is not properly taken into account.

3.4. *One-dimensional scalar spectra*

The quantity usually measured in experiments is the one-dimensional scalar spectrum $E_{1\theta}$ which is related to its three-dimensional counterpart E_θ by the formula

$$E_\theta(k) = -k\frac{\partial E_{1\theta}(k)}{\partial k}, \tag{27}$$

and normalized as

$$\overline{\theta^2} = \int_0^\infty E_{1\theta}(k')\mathrm{d}k' = \int_0^\infty E_\theta(k)\mathrm{d}k, \tag{28}$$

We can obtain the one-dimensional scalar spectrum derived both from the Batchelor and from the Kraichnan three-dimensional spectral forms (9) and (11), respectively:

$$\frac{E_{1\theta}(k)}{\chi(\nu/\epsilon)^{1/2}\eta_B} = q(k\eta_B)^{-1}\,\exp(-q(\eta_B k)^2) + \pi^{1/2}q^{3/2}(\mathrm{erf}(q^{1/2}(\eta_B k)) - 1), \tag{29}$$

$$\frac{E_{1\theta}(k)}{\chi(\nu/\epsilon)^{1/2}\eta_B} = q(k\eta_B)^{-1}\exp(-(6q)^{1/2}\eta_B k). \tag{30}$$

In figure 8 we compare our calculated one-dimensional scalar spectra with the above formulas. The Batchelor k^{-1} range corresponds to the flat part of the curves. Here, as for the previous three-dimensional spectra, Batchelor's prediction agrees fairly well with the simulated data for small k but it diverges for larger wavenumbers ($k\eta_B > 1$), while Kraichnan's model describes the spectrum very well in the entire range of simulated wavenumbers.

3.5. *Location and universality of the k^{-1} range*

The remarkable fact is that Batchelor scaling, originally associated with the properties of high-Reynolds-number turbulence, works so well in our low-Reynolds-number simulations. Batchelor scaling uses the rate of strain of the Kolmogorov eddies $(\epsilon/\nu)^{1/2}$ but one may argue that in our forced simulations the rate of strain of the energy-containing eddies u'/L_p is more appropriate. However, scaling based on u'/L_p did not bring the data to a self-similar form. The success of the Batchelor scaling supports the arguments put forward in the Introduction where we propose that the Batchelor-range spectrum may be independent of Reynolds number because of the universality of the velocity dissipation-range spectrum. It also indirectly supports

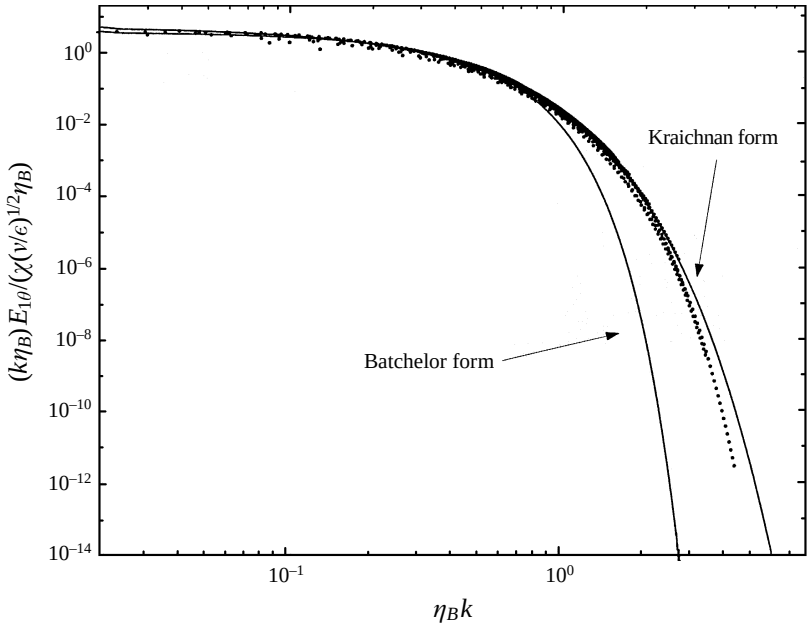

FIGURE 8. Normalized one-dimensional scalar spectra $E_{1\theta}(k\eta_B)(k\eta_B)/(\chi(\nu/\epsilon)^{1/2}\eta_B)$ for all runs and all Prandtl numbers. For comparison the Kraichnan formula (30) and the frequently used Batchelor expression (29) are plotted.

Gibson's (1968*b*) theory which predicts that the Batchelor scaling should apply to the scalar far dissipation range for arbitrary values of Pr, not necessarily for $Pr \gg 1$ as first proposed by Batchelor (1959). The location of the simulated k^{-1} range for $k\eta_B \leqslant 0.2$, equivalent to roughly $k\eta_K \leqslant 1$, appears to be at variance with the Batchelor theory which predicts the k^{-1} range for wavenumbers $k\eta_K \gg 1$. However, the inconsistency is removed if one notes that the velocity scales responsible for the Batchelor-range behaviour should be those that provide the largest rates of strain. Since the spectral estimate of the rate of strain is $(E(k)k^2)^{1/2}$, generally the dominant scales are located in the vicinity of the maximum dissipation wavenumber $k\eta_K \approx 0.2$ rather than around the Kolmogorov wavenumber $k\eta_K \approx 1$. Moreover, the extent and the location of the Batchelor range is consistent with the following Obukhov type argument (Corrsin 1964). The scalar variance flux $F(k)$ at wavenumber k is estimated as

$$F(k) = kE_\theta(k)/\tau(k), \tag{31}$$

where $\tau(k)$ is the turnover time for scales k. In Batchelor's theory the scalar flux and the turnover time are independent of k, $F(k) = \chi$ and $\tau \simeq (\nu/\epsilon)^{1/2}$, respectively, resulting in

$$E_\theta(k) \sim \chi(\nu/\epsilon)^{1/2}k^{-1}. \tag{32}$$

In general the scalar flux is expected to be approximately constant in the range of wavenumbers with negligible scalar variance dissipation. As one progresses towards larger wavenumbers the scalar variance flux is steadily decreased by the dissipation, with the largest effect around the scalar dissipation peak. According to figure 6 the dissipation peak is located somewhere in the range $(0.2 - 0.3)k\eta_B$. Therefore,

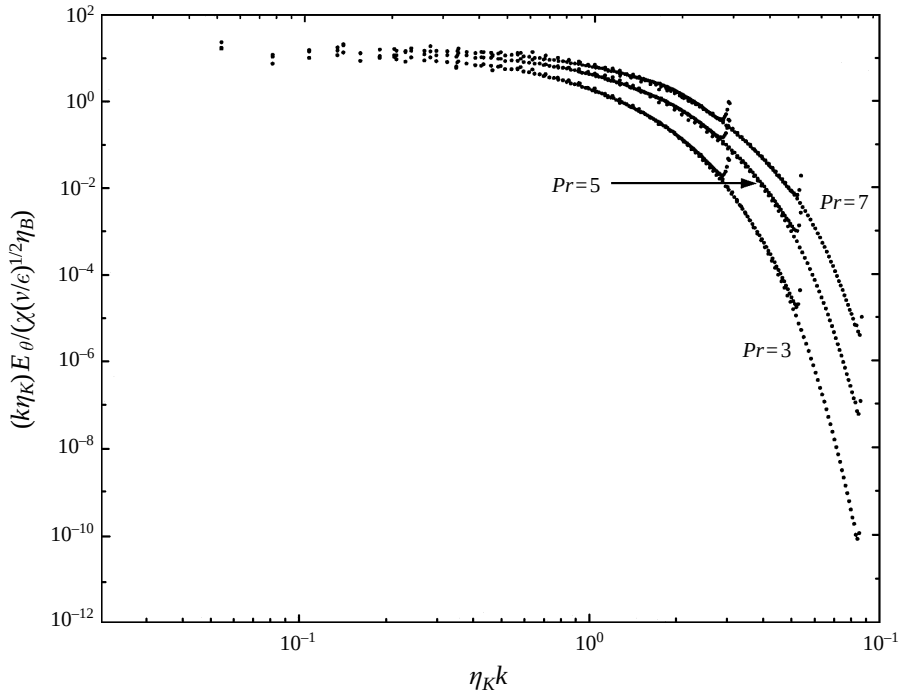

FIGURE 9. Normalized scalar spectra $E_\theta(k\eta_K)(k\eta_K)/(\chi(\nu/\epsilon)^{1/2}\eta_B)$ for all runs and all Prandtl numbers with wavenumbers non-dimensionalized by the Kolmogorov scale.

the previous arguments suggest that the Batchelor range should be observed for $k < 0.2k\eta_B$, which is indeed the case. In general the experimental results are consistent with the onset of the Batchelor range at around $k\eta_K \simeq 0.05$ for Prandtl numbers ranging from $Pr \simeq 1$ to $Pr = 100$ (Hill 1978). In our data the beginning of the k^{-1} range can be observed in figure 9 where the scalar spectra multiplied by k are plotted after normalizing wavenumbers with the Kolmogorov length η_K rather than with the Batchelor length η_B. With this normalization we obtain a family of self-similar curves, one for each different value of the Prandtl number. The extent of the k^{-1} range increases with the increasing value of Pr but all curves converge to a common origin at $k\eta_K \approx 0.05$.

4. Conclusions

We have examined energy and passive scalar spectra obtained in high-resolution direct numerical simulations at three different Reynolds numbers and for three Prandtl numbers $Pr = 3, 5$, and 7.

At the highest Reynolds number $R_\lambda = 77$ the energy spectrum has a short inertial range and the Kolmogorov constant is consistent with experimental data. The lower-Reynolds-number cases do not exhibit the inertial-range behaviour. The maximum in the dissipation spectrum is found between $0.1k\eta_K$ and $0.2k\eta_K$. In all cases the spectra in the far dissipation range for $k\eta_K > 0.2$, i.e. beyond the dissipation peak, have a universal exponential form independent of Reynolds number and with parameters in good agreement with other numerical investigations. The universality implies that those features of turbulence that are determined by scales

from the vicinity of the dissipation peak and beyond can be investigated through direct numerical simulations irrespective of the value of the Reynolds number. In particular, since the Batchelor spectrum for passive scalars with $Pr > 1$ is assumed to be controlled by the velocity scales from the vicinity of $k\eta_K \approx 1$, this suggests that passive scalars with $Pr > 1$ advected by such turbulent velocity fields should exhibit universal behaviour consistent with the predictions of Batchelor (1959) and Gibson (1968*b*).

This conclusion is confirmed by the simulated passive scalar spectra. In all cases we observe the appearance of the Batchelor k^{-1} range followed by the exponential decay in wavenumber k and the spectra are self-similar under the Batchelor scaling. However, we find the Batchelor-range behaviour for wavenumbers $k\eta_K \leqslant 1$, at variance with the Batchelor theory which predicts the k^{-1} range for wavenumbers $k\eta_K \gg 1$. Our results suggest that the velocity scales responsible for the Batchelor-range behaviour reside in the vicinity of the maximum dissipation wavenumber $k\eta_K \approx 0.2$ rather than around the Kolmogorov wavenumber $k\eta_K \approx 1$.

Comparisons with the Batchelor and Kraichnan functional forms of the scalar spectra show that data from our simulations follow closely the Kraichnan form while displaying systematic deviations from the Batchelor form. In the context of oceanographic procedures which estimate the kinetic energy dissipation rates ϵ from the temperature measurements the implication is that the Kraichnan formula will provide more accurate estimates than the Batchelor formula.

Our numerical results contribute to the ongoing discussion concerning the form and universality of passive scalar spectra in turbulent flows for $Pr > 1$. It may be useful to summarize briefly several main differences between our assumptions and experimental conditions and those of other studies since they may responsible for the different conclusion reached. The values of the Prandtl number in the simulations (3, 5, and 7) are greater than unity but much less than those of some experiments (Miller & Dimotakis 1995; Williams *et al.* 1997). Similarly, the values of Reynolds numbers in the simulations are much smaller than in many experiments but comparable to others (Gargett 1985). The simulations are very well resolved in the range of small scales, much better than typical experiments or field measurements (Oakey 1982), allowing the clear distinction between the Gaussian and exponential fall-off at large k. Contrary to other numerical simulations (Pumir 1994) which restrict the velocity field responsible for advecting the scalar to only a few active modes, we use the full velocity field obtained from the Navier–Stokes equations. This may enable us to observe the k^{-1} range at smaller resolutions than suggested by other numerical models.

Finally, we believe that analyses of the velocity and scalar fields using physical space representations are helpful in determining the precise physical mechanisms responsible for the Batchelor-range behaviour and we propose that such analysis be performed in the future.

This work was supported by the ONR Contract No. 00014-94-0107 (Contract Monitor Dr S. G. Ackleson). The simulations were run on the Cray C-90 at the San Diego Supercomputer Center. Local computing facilities in the Aerospace Engineering at USC are supported by the Engineering Research Equipment Grant ESC-9424385 from the National Science Foundation. P.K.Y. is also supported by NSF. We thank Dr Neil Oakey for exhaustive comments on the early version of the manuscript and Dr T. Dickey for helpful discussions. Anonymous reviewers made comments and suggestions that helped to improve the manuscript.

REFERENCES

Antonsen, T. M., Fan, Z. F. & Ott, E. 1995 k spectrum of passive scalars in Lagrangian chaotic fluid flows. *Phys. Rev. Lett.* **75**, 1751–1754.

Batchelor, G. K. 1959 Small scale variation of convected quantities like temperature in a turbulent fluid. *J. Fluid Mech.* **5**, 113–133.

Batchelor, G. K., Howells, I. D. & Townsend, A. A. 1959 Small scale variation of convected quantities like temperature in a turbulent fluid. The case of large conductivity. *J. Fluid Mech.* **5**, 134–139.

Caldwell, D. R., Dillon, T. M., Brubaker, J. M., Newburger, P. A. & Paulson, C. A. 1980 The scaling of vertical temperature gradient spectra. *J. Geophys. Res.* **85**, 1917–1924.

Chasnov, J., Canuto, V. M. & Rogallo, R. S. 1988 Turbulence spectrum of a passive temperature field: results of a numerical simulation. *Phys. Fluids* **31**, 2065–2067.

Chen, S., Doolen, G., Herring, J., Kraichnan, R., Orszag, S. & She, Z. 1993 Far dissipation range of turbulence. *Phys. Rev. Lett.* **70**, 3051–3054.

Clay, J. P. 1973 Turbulent mixing of temperature in water, air and mercury. PhD thesis, University of California at San Diego.

Corrsin, S. 1951 On the spectrum of isotropic temperature fluctuations in isotropic turbulence. *J. Appl. Phys* **22**, 469.

Corrsin, S. 1964 Further generalization of Onsager's cascade model for turbulent spectra. *Phys. Fluids* **7**, 1156–1159.

Dillon, T. M. & Caldwell, D. R. 1980 The Batchelor spectrum and dissipation in the upper ocean. *J. Geophys. Res.* **85**, 1910–1916.

Dimotakis, P. & Miller, P. 1991 Some consequences of the boundedness of scalar fluctuations. *Phys. Fluids* A **3**, 1919–1920.

Domaradzki, J. A. 1992 Nonlocal triad interactions and the dissipation range of isotropic turbulence. *Phys. Fluids* A **4**, 2037–2045.

Gargett, A. 1985 Evolution of scalar spectra with the decay of turbulence in a stratified fluid. *J. Fluid Mech.* **159**, 379–401.

Gibson, C. H. 1968*a* Fine structure of scalar fields mixed by turbulence. I. Zero-gradient points and minimal gradient surfaces. *Phys. Fluids* **11**, 2305–2315.

Gibson, C. H. 1968*b* Fine structure of scalar fields mixed by turbulence. II. Spectral theory. *Phys. Fluids* **11**, 2316–2327.

Gibson, C. H. 1991 Kolmogorov similarity hypotheses for scalar fields: sampling intermittent turbulent mixing in the ocean and galaxy. *Proc. R. Soc. Lond.* A **434**, 149–164.

Gibson, C. H. & Schwarz, W. H. 1963 The universal equilibrium spectra of turbulent velocity and scalar fields. *J. Fluid Mech.* **16**, 365–384.

Grant, H. L., Hughes, B. A., Williams, R. B. & Moilliet, A. 1968 The spectrum of temperature fluctuations in turbulent flow. *J. Fluid Mech.* **34**, 423–442.

Gregg, M. C. 1987 Diapycnal mixing in the thermocline: a review. *J. Geophys. Res.* **92**, 9686–9698.

Herring, J. R. & Kerr, R. M. 1982 Comparison of direct numerical simulations with predictions of two-point closures for isotropic turbulence convecting a passive scalar. *J. Fluid Mech.* **118**, 205–219.

Hill, R. J. 1978 Models of the scalar spectrum for turbulent advection. *J. Fluid Mech.* **88**, 541–562.

Holzer, M. & Siggia, E. D. 1994 Turbulent mixing of a passive scalar *Phys. Fluids* **6**, 1820–1837.

Kerr, R. M. 1985 High-order derivative correlations and the alignment of small-scale structures in isotropic numerical turbulence. *J. Fluid Mech.* **153**, 31–58.

Kerr, R. M. 1990 Velocity, scalar and transfer spectra in numerical turbulence. *J. Fluid Mech.* **211**, 309–332.

Kida, S. & Murakami, Y. 1987 Kolmogorov similarity in freely decaying turbulence. *Phys. Fluids* **30**, 2030–2039.

Kraichnan, R. 1959 The structure of isotropic turbulence at very high Reynolds numbers. *J. Fluid Mech.* **5**, 497–543.

Kraichnan, R. 1968 Small-scale structure of a scalar field convected by turbulence. *Phys. Fluids* **11**, 945–953.

Lesieur, M. 1990 *Turbulence in Fluids.* Kluwer.

Martinez, D., Chen, S., Doolen, G., Kraichnan, R., Wang, L. & Zhou, Y. 1997 Energy spectrum in the dissipation range of turbulence. *J. Plasma Phys.* (in press).

Metais, O. & Lesieur, M. 1992 Spectral large-eddy simulation of isotropic and stably stratified turbulence. *J. Fluid Mech.* **239**, 157–194.

Miller, P. L. & Dimotakis, P. E. 1995 Measurements of scalar power spectra in high Schmidt number turbulent jets. *J. Fluid Mech.* **308**, 129–146.

Mjølsness, R. C. 1975 Diffussion of a passive scalar at large Prandtl number according to the abridged Lagrangian interaction theory. *Phys. Fluids* **18**, 1393–1394.

Monin, A. S. & Yaglom, A. M. 1971 *Statistical Fluid Mechanics: Mechanics of Turbulence.* MIT Press.

Newman, G. R. & Herring, J. R. 1979 A test field study of a passive scalar in isotropic turbulence. *J. Fluid Mech.* **94**, 163–194.

Oakey, N. S. 1982 Determination of the rate of dissipation of turbulent energy from simultaneous temperature and velocity shear microstructure measurements. *J. Phys. Oceanogr.* **12**, 256–271.

Obukhov, A. M. 1949 Structure of the temperature field in turbulent flows. *Isv. Geogr. Geophys. Ser.* **13**, 58–69.

Pumir, A. 1994 Small scale properties of scalar and velocity differences in three-dimensional turbulence. *Phys. Fluids* **6**, 3974–3984.

Qian, J. 1995 Viscous range of turbulent scalar of large Prandtl number. *Fluid Dyn. Res.* **15**, 103–112.

Rogallo, R. S. 1981 Numerical experiments in homogeneous turbulence. *NASA Tech. Mem.* 81315.

Ruetsch, G. R. & Maxey, M. R. 1991 Small - scale features of vorticity and passive scalar fields in homogenous isotropic turbulence. *Phys. Fluids* A **3**, 1587–1597.

Sreenivasan, K. 1985 On the fine-scale intermittency of turbulence. *J. Fluid Mech.* **151**, 81.

Sullivan, N. P., Mahalingam, S. & Kerr, R. 1994 Deterministic forcing of homogeneous, isotropic turbulence. *Phys. Fluids* **6**, 1612–1614.

Tatarski, V. I. 1961 *Wave Propagation in Turbulent Media.* McGraw-Hill.

Tennekes, H. & Lumley, J. L. 1972: *A First Course in Turbulence.* MIT Press.

Williams, B., Marteau, D. & Gollub, J. 1997 Mixing of a passive scalar in a magnetically forced two-dimensional turbulence. *Phys. Fluids* (in press).

Yeung, P. K. & Pope, S. B. 1988 An algorithm for tracking fluid particles in numerical simulations of homogeneous turbulence. *J. Comput. Phys.* **79**, 531–586.